DNA Topology on an Increase in Positive Writhing Number of DNA: Conformation Changes in the Time Course of *cis*-Diamminedichloroplatinum(II)–DNA Adducts

Shigeki Kobayashi,[*,a] Yoshihide Nakamura,[a] Tamae Maehara,[a] Hajime Hamashima,[b]
Masanori Sasatsu,[c] Koji Asano,[d] Yukihiko Ohishi,[d] and Akira Tanaka[a]

*Departments of Analytical Chemistry of Medicines[a] and Microbiology,[b] Showa Pharmaceutical University, 3–3165
Higashi-tamagawagakuen, Machida, Tokyo 194–8543, Japan, Department of Microbiology, School of Pharmacy, Tokyo
University of Pharmacy and Life Science,[c] Tokyo 192–0392, Japan, and Department of Urology, Jikei University School of
Medicine,[d] 3–25–8 Nishi-shinbashi, Minato-ku, 105–8461 Tokyo, Japan.*

We show that the topological significance of the gel mobility of *cis*-diamminedichloroplatinum(II) (DDP)–closed circular DNA (ccDNA) adducts decreases with reaction time, until a point at which it joins relaxed DNA, and that the mobility of the adducts increases again. There is no relationship between the relative length of the adducts and the gel mobility. Although the significance of the decrease of gel mobility is due to the unwinding of *cis*-DDP–DNA (or *trans*-DDP–DNA) adducts, the conformational significance of the subsequent increase in mobility is unclear. To elucidate the conformational significance for unwinding of the adducts, we measured the writhing number (Wk) of the adducts using electron microscopy and analyzed the topological states of *cis*-DDP (or *trans*-DDP) adducts based on the White rule, Lk=Wk+Tk. Where, Lk and Tk represent the linking and twisting number in the ring, respectively. From the data, we found that the Wk of *cis*-DDP–ccDNA adducts in comparison with *trans*-DDP–ccDNA adducts increases from a negative to a positive number with time. This suggests that *cis*-DDP plays a role in the change of the topological state of ccDNA. In the abstraction of platinum from the adducts with CN$^-$ ion, the differences in both topological states may explain why Pt in *trans*-DDP is abstracted more easily than in *cis*-DDP. To explain the abstraction of Pt ion, we also discuss the findings based on the thermodynamic cycle in a intermolecular crosslink model Pt(NH$_3$)$_2$(guanine)$_2^{2+}$→Pt(CN)$_4^{2-}$ using the Pt parametrized PM3 method.

Key words *cis*-diamminedichloroplatinum(II); anticancer therapy; DNA topology; writhing number; White rule; gel electrophoresis

Much attention has been paid by chemists, pharmacologists, and clinicians to the inorganic antitumor drug, *cis*-diamminedichloroplatinum(II) (*cis*-Pt(NH$_3$)$_2$Cl$_2$, *cis*-DDP) (**1**) and other related platinum complex derivatives which are most effective drugs for cancer chemotherapy. Although *cis*-DDP is widely used as a chemotherapeutic agent, the stereoisomer *trans*-diamminedichloroplatinum(II) (*trans*-DDP) (**2**) is inactive.[1] The working mechanism of *cis*-DDP is generally believed to be binding of *cis*-DDP to cellular DNA, and three binding modes have been reported using binding models; i) intermolecular crosslink, ii) intramolecular crosslink, and iii) monofunctional links.[2] Recently, Lippard and his co-workers. reported the structure of synthesized *cis*-DDP–12mer oligo DNA adducts by X ray-crystallography and the DNA is bent, leading to major groove damage to the Watson–Crick hydrogen bonding.[3] In spite of numerous studies of the structure of *cis*- and *trans*-DDP–DNA adducts, the tertiary structural differences are still unknown. The clarification of the tertiary structure of the adducts is essential for considering drug design and the working mechanism of platinum-anticancer drugs.

In the previous paper, we reported that the formation of mainly three unique topologically distinct invariant DNAs, such as dimetric catenane, singly-linked catenane, and trefoiled knot, *etc.* is caused by reaction of DNA topoisomerase I with *cis*-DDP–DNA adducts.[4] We pointed out the importance of formation of intra-twisting looped DNAs, and that *cis*-DDP is a factor that changes the topological invariants of circular closed DNA (ccDNA). To elucidate the binding pathway of *cis*-DDP and *trans*-DDP with closed circular pBR322 DNA, we investigated the topological differences in the time course of the formation of Pt^{2+}–DNA adducts. Although the time course of binding of *cis*-DDP to DNA decreases the electrophoretic mobility of *cis*-DDP–DNA adducts in agarose gel electrophoresis, the mobility increases again with time. Cohen *et al.* previously reported the shortening of closed circular pSM1 DNA.[5] We confirmed that the electrophoretic mobility of linear pBR322 prepared by cutting pBR322 DNA by *Hind*III also changes by *cis*-DDP binding. This indicates that *cis*-DDP changes also the topological properties of linear DNA.

The increase and decrease of the gel electrophoretic mobilities of the *cis*-DDP–ccDNA adducts are repeated in the time course in the gel. To demonstrate the reasons, electron microscopy and White rule[6] were used. The change from decrease to increase is caused by alternation from negative (−) to positive (+) writhing numbers (Wk) for the adducts, and we showed that *cis*-DDP increases the positive writhing number more than *trans*-DDP. These results provide a new key to explain the significant differences in the antitumor activity of *cis*-DDP and *trans*-DDP.

Experimental

Materials The platinum complexes, *cis*-Pt(NH$_3$)$_2$Cl$_2$ and *trans*-Pt(NH$_3$)$_2$Cl$_2$, were purchased from Aldrich Co. (U.S.A.). Closed circular supercoiled pBR322 plasmid DNA was isolated by chloramphenicol amplification of *E. coli* cultures.

Preparation of *cis*-DDP– and *trans*-DDP–pBR322 DNA Adducts Stock solutions of *cis*-DDP and *trans*-DDP (5.0×10^{-3} M) were prepared by dissolving the complex in 0.01 M Tris–HCl buffer (1×TH; pH=7.5). The

cis-DDP– and *trans*-DDP–DNA adducts were prepared by incubation with 0.08 µg of pBR322 DNA for 72, 48, 30, 24, 12, 8, 6, 3, 2, 1, 0.5, 0.25, and 0.0 h at a final concentration of 1.0×10^{-4} M of *cis*-DDP and *trans*-DDP, respectively, in a solution (final volume 10 µl) of 0.01 M TH (pH=7.5) at 37 °C and stored at 4 °C for 3 d in the dark.

Abstraction of Platinum Ion from Pt–DNA Adducts by Cyanide Ion Potassium cyanide (27.4 mg) was dissolved in 0.1 M TH buffer (559 µl, pH=7.5), and a final concentration of 0.65 M was prepared by readjustment to pH 8.5 with 300 µl of 0.01 M TH buffer (pH=3.0). Abstraction of platinum from Pt–DNA adducts was performed by addition 2 µl of 0.1 M TH buffer (pH=7.5) and 3 µl of 650 mM cyanide stock solution and by incubation at 37 °C for 4 h.

Gel Electrophoresis The platinum–DNA adducts were loaded on an 0.8% agarose gel electrophoresis in TBE (0.09 M Tris–borate, 0.002 M EDTA, pH=8.1) buffer at 15 V (1.5 V/cm) constant power for 16 h. The gels were stained with ethidium bromide (0.5 µg/ml) for 1 h in TBE buffer, and photographed under UV with a Polaroid camera using Polapan 665 (or 667) films. The mobility and concentration of DNA on the gel were measured by a Pharmacia Image Analyzer (ImageMaster).

Electron Microscopy The treatment of samples used for electron microscopy was essentially the same as that described by Yamagishi.[7] The grids were inserted into a JEOL JEM-SCAN100CX II electron microscope, so that the shadowed surface, followed by rotary-shadowcasting with tungsten, of the grid faced toward the emulsion side of the sheet film. The contour lengths of platinum–DNA adducts were determined by tracing from negatives of the enlarged image and measured with a digitizer (1200 series graphics calculator, Numonics Corp., PA, U.S.A.).

Simple DNA Topology Linking number (L*k*) of closed circular DNA expresses a topological distinct number. According to White rule,[6] L*k* is the sum of W*k* and twisting number (T*k*).

$$L k = W k + T k \qquad (1)$$

When the ribbon is untwisted; L*k* value is 0, and the ribbon is in relaxed form and T*k* value is equal to W*k* and the value is 0. When the relaxed ribbon is writhed to the left, the right-handed interwound supercoiled ribbon is formed, and T*k*=3, W*k*=−3, and L*k*=0. When the relaxed ribbon is writhed to the right, the left-handed interwound supercoiled ribbon is formed. The ribbons of the right-handed and left-handed supercoil are a negative and a positive sign, respectively. However, native duplex DNA strains have hydrogen bonding between base pairs of both strands; and L*k* is ≠0. For instance, the mean L*k* of closed circular pBR322 plasmid DNA (4361 bp) is 415 where the helical repeat is 10.5 bp/turn, and the DNA underwinds the mean L*k* (<415). Thus, closed circular pBR322 DNA is termed negatively supercoiled. For instance, T*k* of the twisted ribbon of L*k*=10 is +10, and the W*k* value is ≠0. The ribbon of −3 of W*k* has a negative sign, and T*k* is +13. However, the ribbon of +3 of W*k* has a negative sign, and T*k* is 7.

We show the definition of the topological state between intermolecular and intramolecular crosslinks in the *cis*-DDP–ccpBR322 DNA adducts. When the duplexes of *n*=2 and 3 (L*k*=2, 3) are cut lengthwise along the hydrogen bondings between the 5′-to-3′ and 3′-to-5′ direction, the catenane and trefoil are produced, respectively. Similarly, the adducts of *n*=4 (L*k*=4) produce two forms of 4^2_1 catenanes,[8] with a T*k* of 13. By cutting lengthwise, the two adducts show a large difference topologically. This is because, one (not 4^2_1) joins as a bifunctional-bridge with Pt and the other (4^2_1) does not.

Relative Free Energy Difference Optimization of the geometries of platinum complexes, $Pt(NH_3)_2Cl_2$, $Pt(CN)_4^{2-}$,[9] and $Pt(NH_3)_2(guanine)_2^{2+}$ [10] were performed using molecular orbital (MO) methods such as Pt parametrized PM3 Hamiltonians and density functional BLYP/LACVP** implemented in the TITAN software (Wavefunction, U.S.A.). The resultant structures are shown in Fig. 6. The PM3 optimized bond lengths and angles typically differ from literature crystal structures[11] for *cis*-DDP and *trans*-DDP by about 0.017—0.036 Å, 9.70—11.23° and 0.03—0.052 Å and 1.5°, respectively. However, no electronic structure and geometry for the most important chelation of the two guanine residues, $Pt(NH_3)_2(guanine)_2^{2+}$, within DNA adducts d(G/G) by *cis*-DDP have been reported.

The relative free energy difference between *cis*-$Pt(NH_3)_2(guanine)_2^{2+}$ (**3**) and *trans*-$Pt(NH_3)_2(guanine)_2^{2+}$ (**4**) was calculated using the thermodynamic cycle, as shown in Chart 1. The relative free energy of association ($\Delta\Delta G = \Delta G_{trans} - \Delta G_{cis}$) was obtained by calculation of $\Delta G_1 + \Delta G_2 - \Delta G_3 - \Delta G_4 = \Delta G_1 = \Delta\Delta G$ (because $\Delta G_2 = \Delta G_3 = \Delta G_4 = 0$). The free energy ΔG values are given by $H - T\Delta S$ (*H*; enthalpy, *T*=absolute temperature (K), and *S*=entropy), and these *H* and ΔS values were obtained from the calculated thermodynamic properties of the target compounds.

Results

Electrophoretic Mobilities of *cis*-DDP– and *trans*-DDP–Close Circular pBR322 DNA Adducts and *cis*-DDP–Supercoiled DNA Adducts *cis*-DDP– and *trans*-DDP–DNA adducts were prepared by incubation with DNA (0.08 µg) in the presence of freshly prepared *cis*-DDP and *trans*-DDP (1×10^{-4} M) in 0.01 M, TH buffer (pH=7.5) solution at 37 °C, respectively, and the reactions were stopped by addition of 2 µl of 1.0 M NaCl solution. The results of agarose gel electrophoretic analysis with pBR322 DNA and platinum complexes are summarized in Fig. 1. The electrophoretic mobilities of supercoiled DNA decrease with reaction time (t_1). After 1 h of reaction time, a drastic change in mobility was observed, and the band overlapped with the relaxed form of DNA. The increase and decrease of the mobilities were repeated in time course in the gel.

Figure 1 shows the electrophoretic mobilities as a function of incubation time of pBR322 DNA with *cis*-DDP (log 1/M) (or *trans*-DDP). These graphics show the difference of interaction with DNA between *cis*-DDP and *trans*-DDP. The electrophoretic mobilities of *cis*-DDP–DNA adducts decrease as
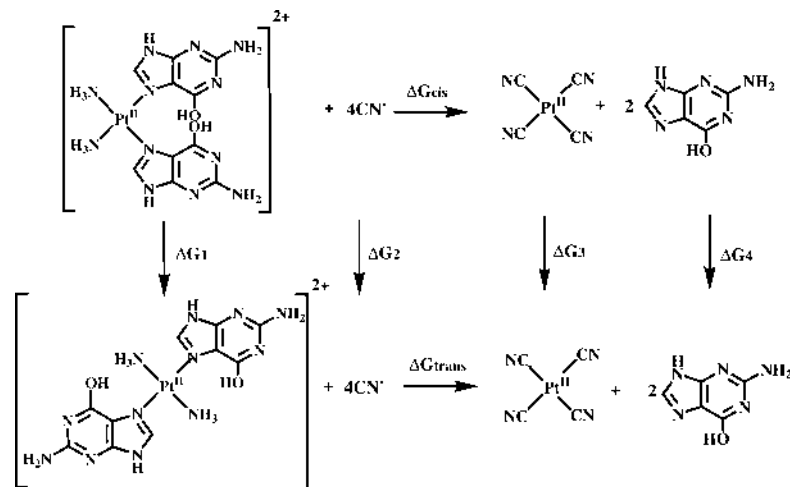

Chart 1. Thermodynamic Cycle for the Reaction from Intermolecular Crosslink Model *cis/trans*-Pt(guanine)$_2$(NH$_3$)$_2^{2+}$ to Pt(CN)$_4^{2-}$

$\Delta G_{cis/trans}$ represents free energy differences for reactions of *cis/trans*-Pt^{2+} ions with CN$^-$ ion (in the gas phase).
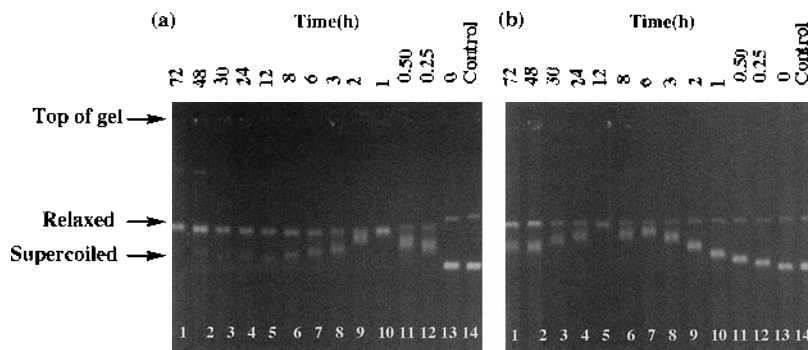
Fig. 1. Time Course of Agarose Gel Electrophoresis of *cis* (or *trans*)-DDP–pBR322 DNA Adducts Produced by Reaction of pBR322 DNA with *cis* (or *trans*-)-DDP

(a) *cis*-DDP (final concentration; 1.0×10^{-4} M)–pBR322 DNA (0.08 μg) and (b) *trans*-DDP–pBR322 DNA adducts.

incubation time increases and overlap with relaxed form DNA after about 1 h. Later, the mobilities increase again. Furthermore, the mobilities of *cis*-DDP–relaxed form DNA adducts increase as incubation time increases and reach a maximum after 6 h (lane 7 in Fig. 1a). The mobilities repeat the decrease, and overlap with relaxed form DNA. However, the bands of *trans*-DDP–DNA adducts overlap with relaxed form DNA adducts after about 12 h and the mobilities increase later. Interestingly, the mobilities of *trans*-DDP–relaxed form DNAs show almost no changes, but the mobilities of *cis*-DDP–DNA adducts repeat the change in the gel. Moreover, the binding of *cis*-DDP to DNA reduces the ability to visualizes DNA stained with ethidium bromide in the gel.

Electrophoretic Mobilities of Abstraction of Platinum Ion from *cis*-DDP–DNA Adducts by Cyanide Ion Figure 2 shows the electrophoretic mobilities of the products incubated with *cis*-DDP–DNA (or *trans*-DDP) adducts of 0.2 M KCN at 37 °C for 4 h in 0.01 M TH buffer (pH=7.5). After incubation, the mobilities of *trans*-DDP–DNA adducts (lanes 6—10 in Fig. 2) were consistent with the mobility of the control supercoiled DNA. Although the mobilities of both *cis*-DDP–DNA adducts and control ccDNA are consistent within 0.25 h incubation time, a later times the mobilities did not agree (lanes 1—3). The mobility of *cis*-DDP–DNA adducts by incubation of DNA with *cis*-DDP for 8 h decreases after 3 h, as shown in Fig. 2 (lanes 1, 2). This finding shows that the conformational structure of *cis*-DDP–DNA adducts changes by cleavage of the N–Pt bond, and it is possible that DNA cisplatination is consistent with transformation from negative supercoiled DNA to positive supercoiled DNA. Moreover, the Pt^{2+}–N bond of *trans*-DDP–DNA is a weaker bond than that of *cis*-DDP–DNA adducts. Although the weak platinum binding is a coordination link, *trans*-DDP is easily removed from DNA by abstraction of Pt^{2+} ion with CN^- ions.

Length Measurement of *cis*-DDP– and *trans*-DDP–Closed Circular pBR322 DNA Adducts It is believed that the increase and decrease of mobilities of the adducts is related to partially collapsed DNA. We found that the changes are related to changes in the writhing number (W*k*) of DNA by electron photographs of *cis*-DDP– and *trans*-DDP–pBR322 DNA adducts. Figures 3 and 4 show distribution histograms of the lengths of the *cis*-DDP–DNA and *trans*-DDP–DNA adducts. The mean length of pBR322 DNA was
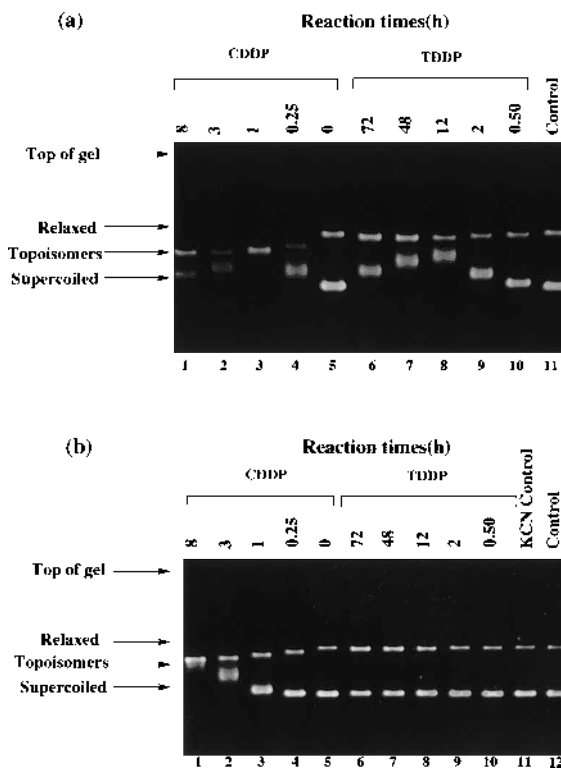

Fig. 2. Effect of Abstraction by CN^- Ion of Platinum Ion Bound with DNA in *cis*-DDP–DNA and *trans*-DDP–DNA Adducts

(a) Time course of *cis*-DDP or *trans*-DDP (final concentration; 1.0×10^{-4} M)–pBR322 DNA (0.08 μg) adducts produced by reaction of *cis*-DDP or *trans*-DDP with pBR322 DNA. (b) Gel bands of DNA produced by reaction of CN^- with *cis* (or *trans*-)-DDP–pBR322 DNA adducts produced during the time course of the reaction.

1.370 μm ($n=200$), and the mean length of *cis*-DDP–DNA adducts was 1.036 μm ($n=252$) at 0.25 h incubation, and the mean lengths were 0.939 μm ($n=267$) and 0.998 μm ($n=319$) length after 2 and 12 h incubation, respectively. As a result, it is clear that DNA length shortened by binding with *cis*-DDP. At 72 h incubation, however, the mean length of the *cis*-DDP–DNA adducts increased to 1.043 μm ($n=292$), and the increased gel mobilities were decreased. The increase or decrease in mobility indicates the periodical difference in the structure of *cis*-DDP–DNA adducts.

On the other hand, the mean lengths of *trans*-DDP–DNA adducts were 1.084 μm ($n=245$), 1.110 μm ($n=269$), 1.124 μm ($n=274$), and 1.102 μm ($n=279$) at 0.5, 3, 24, and 72 h
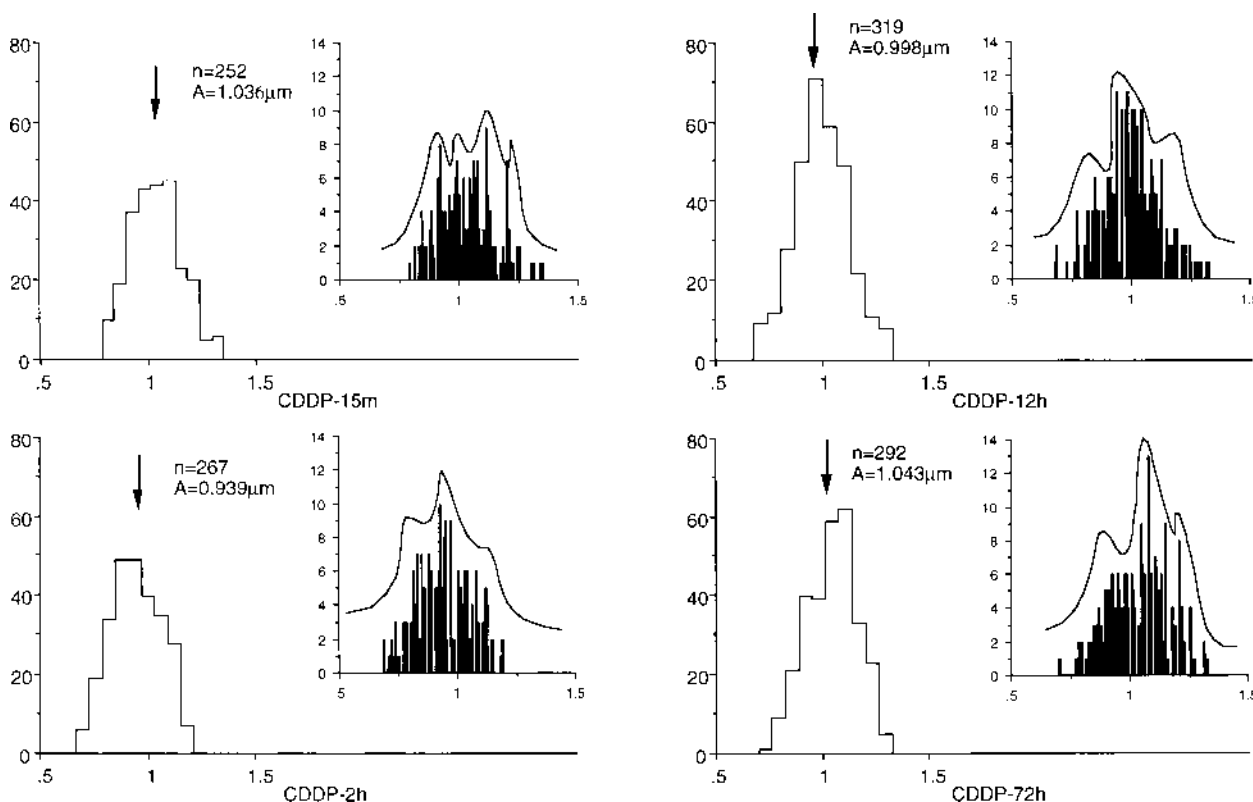
Fig. 3. Distribution of Contour Lengths of *cis*-DDP–DNA Adducts Produced by Reaction of *cis*-DDP with pBR322 DNA

Figure presents contour lengths of *cis*-DDP–DNA adducts after the reaction times 0.25, 2, 12, and 72 h. Length (μm) is indicated on the abscissa and the number (*n*) of DNA molecules is the ordinate. The mean length is indicated with an arrow on the graph; 0.25 h, 1.036 μm (*n*=252 molecules measured); 2 h, 0.939 μm (*n*=267); 12 h, 0.998 μm (*n*=319); 72 h, 1.043 μm (*n*=292), respectively. CDDP: *cis*-DDP.
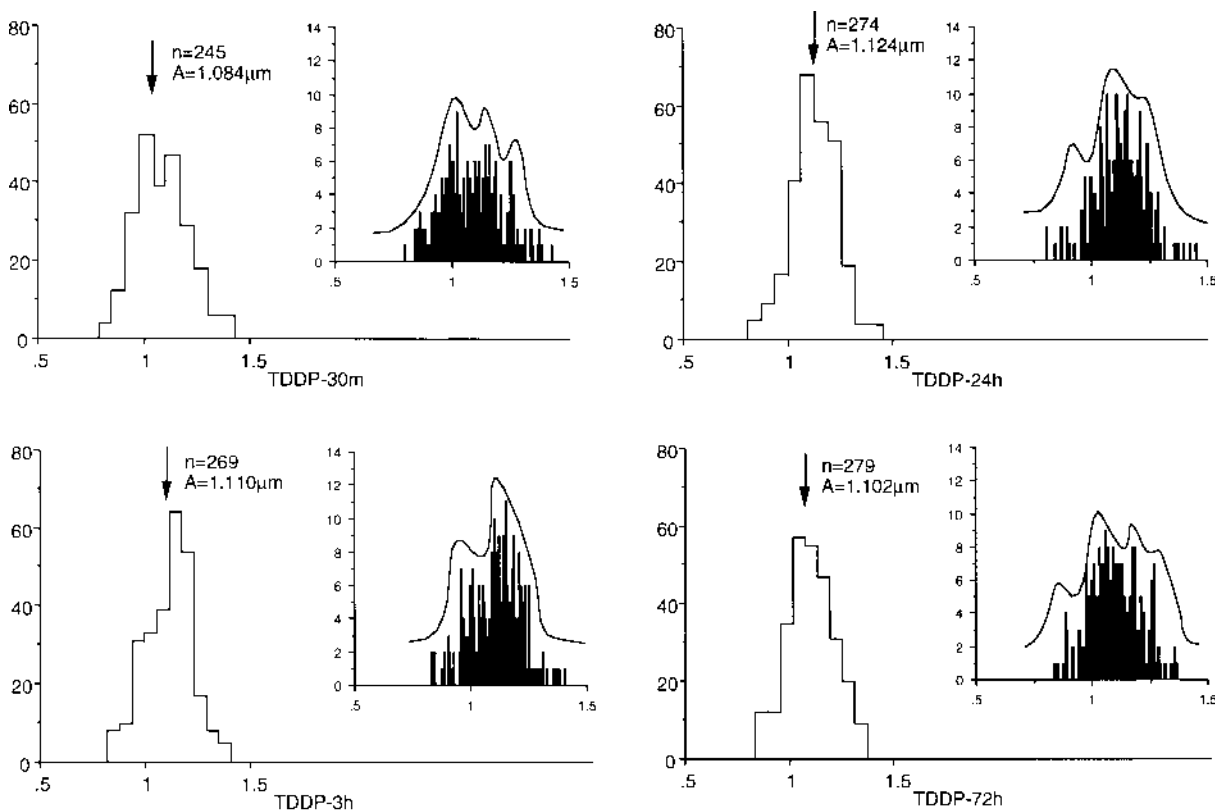

Fig. 4. Distribution of Contour Lengths of *trans*-DDP–DNA Adducts Produced by Reaction of *trans*-DDP with pBR322 DNA

Figure presents the contour lengths of *trans*-DDP–DNA adducts as a function of reaction time; 0.5, 3, 24, and 72 h. Length (μm) is indicated by the abscissa and the number (*n*) of DNA molecules is indicated by the ordinate. The mean length is indicated with an arrow on the graph; 0.5 h, 1.084 μm (*n*=245 molecules measured); 3 h, 1.110 μm (*n*=269); 24 h, 1.124 μm (*n*=274); 72 h, 1.102 μm (*n*=279), respectively. TDDP: *trans*-DDP.

incubation, respectively. Accordingly, the *trans*-DDP–DNA adducts are about 1.08—1.12 μm length, and it is seen that the mean lengths do not show large differences in the time course. The mean lengths are longer than the length of the *cis*-DDP–DNA adducts. Obviously, there is a relationship between the mean length and gel mobility of the adducts, since the gel mobility of *cis*-DDP–DNA adducts (after reaction of 0.25 h) is equal to that of the adducts (after reaction of 72 h).

Measurement of Writhing Number of *cis*-DDP– and *trans*-DDP–DNA Adducts by Electron Photography To elucidate the cause of the reversible increase in electrophoretic mobility, we applied a simple topological method to *cis*-DDP– and *trans*-DDP–DNA adducts, since the cause may be related to the geometric conformation of binding of *cis*-DDP or *trans*-DDP to DNA, leading to changes in local linking number (ΔLk) and supercoiling of closed circular DNA.

Figure 5 shows typical electron micrographs defined with writhing number, of *cis*-DDP adducts produced by incubation at 37 °C for 72 h. Although pBR322 DNA is negative supercoiled DNA, the positive unwind (b) and intra-twisted looped forms (c) increase by binding of *cis*-DDP. The sign convention for circular closed supercoiled DNA crossings is illustrated in Fig. 5d.[12] Accordingly, the Wk of the adducts ((a), (b), and (c) in Fig. 5) were assigned to -1, $+1$, and -1, respectively, for curve crossings.

The measurements of Wk were performed using electron microscopy, and the results are summarized in Tables 1 and 2. The gel band of *cis*-DDP–DNA adducts after a reaction time of 72 h are shown in lane 1 in Fig. 1a. The mean writhing number of the adducts was $+0.75$. After a reaction time of 0.5 h, the mean writhing number of the *cis*-DDP–DNA adducts was -1.03. The mean writhing number
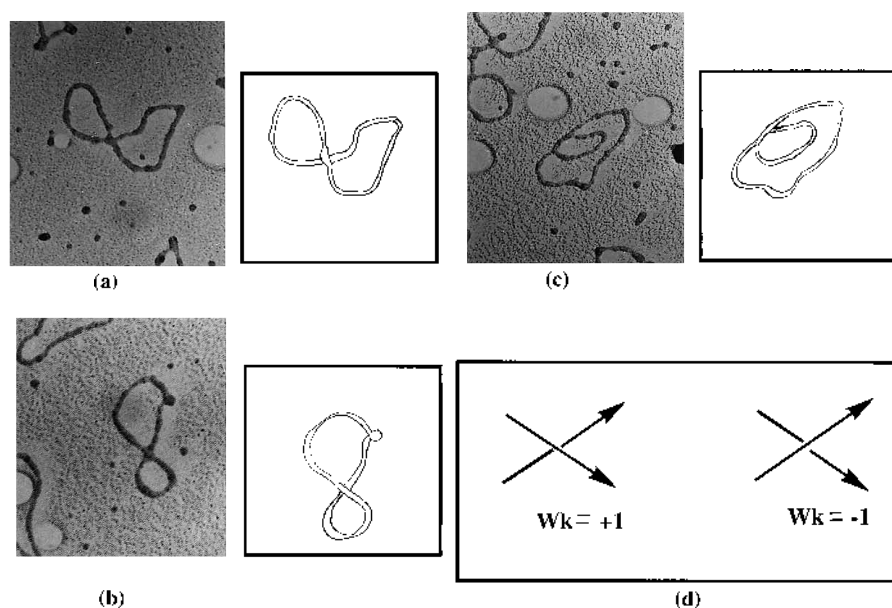

Fig. 5. Electron Micrographs of *cis*-DDP–pBR322 DNA Adducts and Writhing Numbers

The representations of *cis*-DDP–DNA isomers incubated for 72 h are (a) W$k=-1$, (b) W$k=+1$, (c) W$k=-1$, respectively. (d) Sign convention for ribbon crossings. Clockwise and anticlockwise motion define ($-$) and ($+$) crossings, respectively.

Table 1. Determination of Writhing Number in Time Course for *cis*-DDP–pBR322 DNA Adducts

| Compounds | Reaction time (h) | Wk (writhing number) | | | | | | | | Number | | |
		+4	+3	+2	+1	−1	−2	−3	−4	Positive l supercoi	Negative supercoil	$\dfrac{P}{P+N}$
Cisplatin	72	2	15	43	74	43	7	5	0	134	55	71%[a]
(*cis*-DDP)	0.5	0	2	3	12	21	19	12	0	17	52	25%

a) (P/P+N)×100=(134/134+55)×100=71%.

Table 2. Determination of Writhing Number in Time Course for *trans*-DDP–pBR322 DNA Adducts

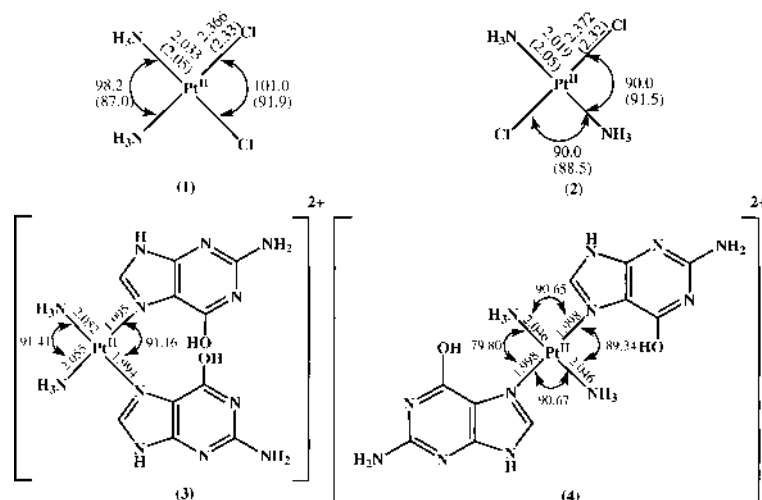| Compounds | Reaction time (h) | Wk (writhing number) | | | | | | | | Number | | |
		+4	+3	+2	+1	−1	−2	−3	−4	Positive supercoil	Negative supercoil	$\dfrac{P}{P+N}$
Transplatin	72	0	4	16	18	11	15	5	0	38	31	55%[a]
(*trans*-DDP)	0.5	1	0	15	9	17	18	4	1	25	40	38%

a) (P/P+N)×100=(38/38+31)×100=55%.

Fig. 6. Optimized Geometries of *cis/trans*-DDP, Intermolecular Crosslink Model, *cis/trans*-Pt(guanine)$_2$(NH$_3$)$_2$, Using a Pt parametrized PM3 Method

The values in parentheses for *cis*- and *trans*-DDP are data taken from the literature.[11]

of the Pt–DNA adducts is dependent not only on the reaction time but also *cis*- (or *trans*)-DDP. The mean writhing number of *trans*-DDP–DNA adducts was +0.10 after a reaction time of 72 h. It was found that the transformation from negative DNA to positive DNA by *trans*-DDP is weak. As a result, the unwinding of DNA by *cis*-DDP originates from an increase in positive writhing number.

Thermodynamics of *cis/trans* Pt(guanine)$_2$(NH$_3$)$_2^{2+}$→ Pt(CN)$_4^{2-}$ Pathway The Pt parametrized PM3 and BLYP/LACVP** optimized geometry of *cis*-DDP and *trans*-DDP were fitted to the experimental data. From the gel electrophoresis data (Fig. 2), it is clear that the *cis*-DDP in *cis*-DDP–DNA adducts is bound more strongly than *trans*-DDP. To elucidate these findings, we calculated the free energy differences of the *cis/trans* Pt(guanine)$_2$(NH$_3$)$_2^{2+}$→ Pt(CN)$_4^{2-}$ system, as presented in the thermodynamic cycle (Chart 1) and the interaction energies for *cis/trans* Pt(guanine)$_2$(NH$_3$)$_2^{2+}$→Pt(CN)$_4^{2-}$ transformation using the PM3 hamiltonian. The calculated geometry for the most important chelation of the two guanine residue models, *cis/trans*-Pt(NH$_3$)$_2$(guanine)$_2^{2+}$, is presented in Fig. 6. The relative free energy of association ($\Delta\Delta G = \Delta G_{trans} - \Delta G_{cis}$) was obtained as ΔG_1 and the calculated ΔG_{cis} and ΔG_{trans} values were -61.507 and -60.616 kcal/mol, and was determined to be *ca.* $+1.0$ kcal/mol at the PM3 level. A positive sign means that the *trans*-Pt(NH$_3$)$_2^{2+}$ ion in the *trans*-Pt(NH$_3$)$_2$(guanine)$_2^{2+}$ complex is more easily released from DNA than the *cis*-Pt(NH$_3$)$_2^{2+}$ ion. Similarly, the substitution energies (ΔSE) for guanine→CN$^-$ substitution between Pt(CN)$_4^{2-}$ and *cis/trans* Pt(guanine)$_2$(NH$_3$)$_2^{2+}$ obtained by calculation of the difference $\Delta E_{Pt(CN)_4} - \Delta E_{cis/trans\text{-}Pt(guanine)_2(NH_3)_2}$, were -323.0 and -313.4 kcal/mol, respectively. This also means that *trans*-Pt(NH$_3$)$_2^{2+}$ ion is more easily abstracted from bound DNA bases than *cis*-Pt(NH$_3$)$_2^{2+}$ ion by the addition of CN$^-$ ion.

Discussion

We discovered a reason for the observation of an increase and decrease in gel mobility of *cis*-DDP–DNA adducts over time. We demonstrated using electron micrographs and the White rule that the positive (+) writhing number of the adducts increases. That is, the mobility of *cis*-DDP–DNA adducts decreases with time until the point at which it joins relaxed DNA (lanes 10—13, Fig. 1a), and the mobility of the band then increases again (lanes 1—9, Fig. 1a). What is the chemical significance of the observation that the gel mobility of *cis*-DDP (or *trans*-DDP)–DNA adducts is equal? To understand the significance of the same mobility of the two bands (lanes 8 and 11, Fig. 1a), we measured the topological invariant of a curve, the writhing number, of the Pt^{II}–DNA adducts using electron microscopy. Although the mobility decreases in proportion to the reaction time until the point at which it joins relaxed DNA, and then increases again, the relative length of the adducts shortens in the time course and then lengthens again. For example, we found out that *cis*-DDP–DNA adducts increase from 0.939 μm to 1.043 μm mean length at 2 and 72 h incubation (*cis*-DDP-2 and -72 h in Fig. 3). Interestingly, the mobility of the bands in lanes 1 and 11 (or lanes 8 and 11—12, *etc.*) is the same value (Fig. 1a) and we found a difference in topology between the adducts in lanes 1 and 11 in terms of +W*k* and −W*k* number. *cis*-DDP causes unwinding and winding of supercoils in the time course and plays an important role in the change of DNA writhing number in comparison with *trans*-DDP.

Although the twisting number cannot be observed, the writhing number is possibly observed as described in the section "simple DNA topology." On the changing of the writhing number of Pt^{II}–DNA adducts formed by binding of platinum with pBR322DNA, we found an increase in positive writhing number of platinum–DNA adducts, as listed in Table 1. When pBR322 DNA was incubated for 0.5 h in the presence of *cis*-DDP (1.0×10^{-4} M), the ratio of positive writhing number was 24.6%, and increased to 71% after 72 h incubation. The unwinding of negative supercoiled DNA is caused by *cis*-DDP binding to DNA, and positive supercoiled DNA is produced by excess *cis*-DDP binding, as shown in Fig. 1. The results show that the positive writhing number increases by binding of *cis*-DDP with DNA (see Table 1), hence *cis*-DDP induces an increase of positive writhing number of DNA.

From Eq. 1, the T*k*′ of *cis*-DDP–ccDNA adducts is defined by

$$Tk'\left(\left|\begin{smallmatrix}\rangle\\\langle\end{smallmatrix}\right|\right)=Tk\left(\binom{\cap}{\cup}\right)+n\left(-\Delta Tk\left(\left|\begin{smallmatrix}\rangle\\\langle\end{smallmatrix}\right|\right)\right) \tag{2}$$

here, by $Lk'=Wk'+Tk'$, appearance Lk' is written as

$$Lk'=Wk'+Tk'\left(\left|\begin{smallmatrix}\rangle\\\langle\end{smallmatrix}\right|\right)=Wk'+Tk\left(\binom{\cap}{\cup}\right)+n\left(-\Delta Tk\left(\left|\begin{smallmatrix}\rangle\\\langle\end{smallmatrix}\right|\right)\right) \tag{3}$$

Although $Lk=Lk'$, the mean length of *cis*-DDP–ccDNA adducts is shortened from 1.036 to 0.998 μm in the time course study (see Fig. 3).

Then

$$Wk'-Wk=-\Delta Tk>0 \tag{4}$$

The closed circle $\binom{\cap}{\cup}$ and broken lines $\left(\left|\begin{smallmatrix}\rangle\\\langle\end{smallmatrix}\right|\right)$ show closed circular DNA and partial structures of *cis*-DDP binding with DNA, respectively, and $\left(\left|\begin{smallmatrix}\rangle\\\langle\end{smallmatrix}\right|\right)$ expresses DNA topology of the *cis*-DDP–ccDNA adducts. The action of *cis*-DDP changes the sign of the writhing number from negative to positive. The action of *cis*-DDP resulted in a decrease in the twisting number in comparison with that of *trans*-DDP. That is, the negative sign of ΔTk changes to a positive sign. In fact, the relationship of Wk(*cis*-DDP)$>Wk$(*trans*-DDP) was deduced from the experimental results.

We reported the reaction of DNA topoisomerase I with *cis*-DDP–intra-twisted looped DNA adducts.[4] The writhing number of intra-twisted looped DNA transformed from ccDNA by treatment with *cis*-DDP is discussed. The Tk' of *cis*-DDP–intra-twisted looped DNA adducts also is similarly defined by

$$Tk'\left(\left|\begin{smallmatrix}8\end{smallmatrix}\right|\right)=Tk\left(\left|\begin{smallmatrix}8\end{smallmatrix}\right|\right)+n\left(-\Delta Tk\left(\left|\begin{smallmatrix}|\\|\end{smallmatrix}\right|\right)\right) \tag{5}$$

When Wk is equal to 2, we obtain Eq. 5. Here, by $Lk'=Wk'+Tk'$, the appearance Lk' is written as

$$Lk'=Wk'-2+Tk'\left(\left|\begin{smallmatrix}8\end{smallmatrix}\right|\right)=Wk'-2+Tk\left(\left|\begin{smallmatrix}8\end{smallmatrix}\right|\right)+n\left(-\Delta Tk\left(\left|\begin{smallmatrix}|\\|\end{smallmatrix}\right|\right)\right) \tag{6}$$

As $Lk=Lk'$ generally,

$$n\left(-\Delta Tk\left(\left|\begin{smallmatrix}|\\|\end{smallmatrix}\right|\right)\right)+m=0 \tag{7}$$

Then, as the Tk number of *cis*-DDP DNA adducts is of positive sign, from the experimental data, and Eq. 8 is obtained.

$$n\left(-\Delta Tk\left(\left|\begin{smallmatrix}|\\|\end{smallmatrix}\right|\right)\right)=-m \tag{8}$$

If the sign of m is positive, DNAs bound with *cis*-DDP are positive superhelical braids. Accordingly, the intra-twisted looped DNA also has a positive sign by binding of *cis*-DDP.

Platinum anticancer drugs which increase the writhing numbers to more positive values may be meaningful drugs as chemotherapeutic agents, while chemotherapeutically inactive *trans*-DDP may have a more readily abstracted Pt than in the case of *cis*-DDP (Fig. 2), and we showed by agarose gel electrophoretic mobility of DNA bands that *trans*-DDP was abstracted more easily than *cis*-DDP from Pt–DNA adducts in the presence of CN$^-$ ion. The chemical nature of the complexes such as *cis*-Pt(NH$_3$)$_2^{2+}$, *trans*-Pt(NH$_3$)$_2^{2+}$, *cis*-Pt(guanine)$_2$(NH$_3$)$_2^{2+}$ **3**, and *trans*-Pt(guanine)$_2$(NH$_3$)$_2^{2+}$ **4** is poorly understood yet. To elucidate the differences between *cis*-DDP and *trans*-DDP from the view point of chemotherapy, we calculated the thermodynamic energy and interaction energy for the reaction of the optimized species, since these species are active intermediates for binding with DNA bases.

In the thermodynamic cycle in Chart 1, the free energy differences (ΔG) for i) *cis*-Pt(guanine)$_2$(NH$_3$)$_2\rightarrow$Pt(CN)$_4^{2-}$ and ii) *trans*-Pt(guanine)$_2$(NH$_3$)$_2\rightarrow$Pt(CN)$_4^{2-}$ complexes by
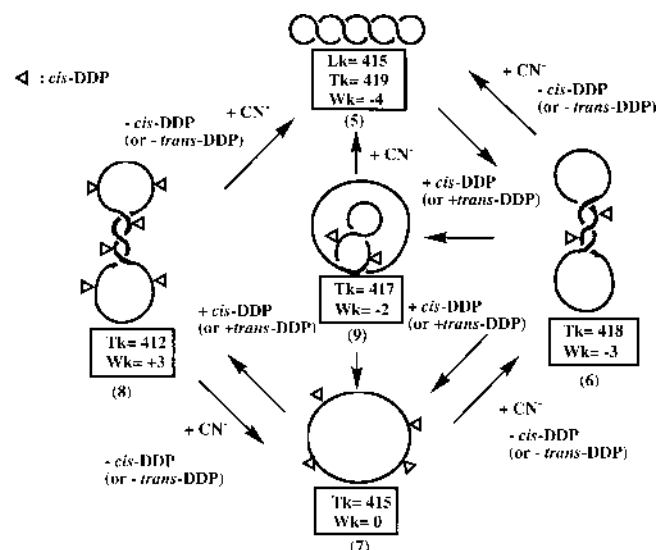

Fig. 7. Illustration of Topological Pathway of *cis*-DDP (or *trans*-DDP)–DNA Adducts

The negative super helical ring (**5**: $Lk=415$, $Tk=+419$, and $Wk=-4$) is shown as an example. The gel mobility of adducts **6** is equal to that of **8**; for instance, see Fig. 1a (lanes 8 and 12, *etc.*).

PM3 level calculation were *ca.* -323.0 and -313.4 kcal/mol, respectively. The relative free energy of association *ca.* 1.0 kcal/mol ($\Delta\Delta G=\Delta G_{trans}-\Delta G_{cis}$) was obtained, since the sign of ΔG_{cis} is positive in reaction ii. Moreover, the interaction energies of *cis*-Pt(NH$_3$)$_2$Cl$_2\rightarrow$*cis*-Pt(guanine)$_2$(NH$_3$)$_2$ and *trans*-Pt(NH$_3$)$_2$Cl$_2\rightarrow$*trans*-Pt(guanine)$_2$(NH$_3$)$_2$ were also calculated, and were -268.8 and -275.6 kcal/mol, respectively. The results suggest that *cis*-Pt(NH$_3$)$_2$Cl$_2$ strongly binds with guanine and that the coordinated guanine of *trans*-Pt(guanine)$_2$(NH$_3$)$_2$ is more easily replaced by CN$^-$ ion than *cis*-Pt(guanine)$_2$(NH$_3$)$_2$. Therefore, Pt–guanine bound in *cis*-Pt(guanine)$_2$(NH$_3$)$_2$ is bound stronger than that in *trans*-Pt(guanine)$_2$(NH$_3$)$_2$ and this can explained the results of the agarose gel experiments. Figure 7 shows the pathway of the topological transformation of *cis*-DDP adducts of superherical duplex, as suggested from the experimental results. For instance, the negative duplex **5** (for example; $Lk=415$, $Tk=+419$, and $Wk=-4$) is unwound by reaction with *cis*-DDP, and transforms to the positive duplex **8** ($Tk=+412$ and $Wk=+3$) corresponding to the binding amount of *cis*-DDP. After reaction with CN$^-$, platinum ion is easily abstracted from the adducts, and the conformation reverses to the starting structure **5**. As a result, the Wk number also reverses to the original number in the *cis*-DDP binding cycle.

Conclusion

We found herein an increase of the writhing numbers of *cis*-DDP–ccDNA adducts in a time course study. Although it is known that the binding of *cis*-DDP shortens the length of DNA, the nature of the Pt^{2+}–DNA adducts was unknown. By binding of *cis*-DDP with DNA, the writhing number of *cis*-DDP–DNA adducts alters from negative to positive. That is, the exact significance of *cis*-DDP-mediated unwinding means that the positive writhing number of negative ccDNAs (pBR322 DNA, *etc.*) increases. This means that *cis*-DDP can change the topological variables, Lk and Wk, of DNA by binding with DNA. The topological states of *cis*-DDP–DNA

adducts differ from the adducts of *trans*-DDP in terms of writhing number and abstraction of Pt ion, and the topological state is related to the degree of abstraction of Pt ion from the *cis*- or *trans*-DDP–adducts. From the thermodynamic cycle of the cross-link models, *cis*-Pt(guanine)$_2$(NH$_3$)$_2 \rightarrow$ Pt(CN)$_4^{2-}$ and *trans*-Pt(guanine)$_2$(NH$_3$)$_2 \rightarrow$Pt(CN)$_4^{2-}$, it is clear that *trans*-DDP is more easily abstracted than *cis*-DDP. The topological proofs of the *cis*-DDP–DNA adducts shown in this paper may be meaningful for the design of very useful platinum complexes as anti-cancer drugs. Further investigations on the topology of *cis*-DDP– and *trans*-DDP–DNA adducts should continue to provide insight at the cell level.

References and Notes

1) *a*) Eastman A., *Pharmacol. Ther*., **34**, 155—166 (1987); *b*) Reedijk J., *Pure Appl. Chem*., **59**, 181—192 (1987); *c*) Sip M., Schwartz A., Vovelle F., Ptak M., Leng M., *Biochemistry*, **31**, 2508—2513 (1992).
2) Kelman A. D., Buchbinder M., *Biochimie*, **60**, 893—899 (1978).
3) Takahara P. M., Rosenzwelg A. C., Frederick C. A., Lippard S. J., *Nature* (London), **377**, 649—652 (1995).
4) Kobayashi S., Furukawa M., Dohi C., Hamashima H., Arai T., Tanaka A., *Chem. Pharm. Bull*., **47**, 783—790 (1999).
5) *a*) Cohen G, Bauer W. R.,Barton J. K., Lippard S. J., *Science*, **203**, 1014—1016 (1979); *b*) Ushay H. M., Tullius T. D., Lippard S. J., *Biochemistry*, **20**, 3744—3748 (1981); *c*) Peritz A., Al-Baker S., Vollano J. F., Schuring J. E., Bradner W. T., Dabrowiak J. C., *J. Med. Chem*., **33**, 2184—2188 (1990); *d*) Seki S., Hongo A., Zhang B., Akiyama K., Sarker A. H., Kudo T., *Jpn. J. Cancer Res*., **84**, 462—467 (1993).
6) *a*) White J. H., *Amer. J. Math*., **91**, 693—728 (1969); *b*) Podtelezhnikov A. A., Cozzarelli N., Vologodskii A., *PNAS*., **96**, 12974—12979 (1999).
7) Yamagishi H., "Chemistry of Nucleic Acid II," ed. by The Japanese Biochemical Society, Tokyo Kagaku Dojin, Tokyo 1989, p. 389.
8) The number expresses a Rolfsen notation. Rolfsen D., "Knots and Links," Publish or Perish Inc., Wilmington, DE, 1976. A Rolfsen notation of closed circular DNA in the text is derived from the theory of the Knot and Link in the representation of the curve. For example, in Rolfsen notation, 2_1^2, the first number 2 is the number of nodes and the superscript is the number of catenated rings, and the script number 1 distinguishes curves with the same number of nodes. Accordingly, the curve of 2_1^2 represents a catenane. When 3_1 is used without superscript, its curve represents only a knot.
9) Bauer W., Gonias S. L., Kam S. K., Wu K. C., Lippard S. J., *Biochemistry*, **17**, 1060—1068 (1978).
10) Fichtinger-Schepman A. M. J., van der Veer J. L., den Hartog J. H. J., Lohman P. H., Reedijk J., *Biochemistry*, **24**, 707—713 (1985).
11) Kelman A. D., Peresie H. J., *Cancer Treat. Rep*., **63**(9—10), 1445—1452 (1979).
12) White J. H., Cozzarelli N. R., *PNAS*., **81**, 3322—3326 (1984).